Supporting information for:

Superior Relaxation of Stresses and Self-Healing Behavior of Epoxy-Amine Coatings

Maurizio Villani [*], *Yogesh S. Deshmukh*, *Caghan Camlibel*, *Catarina Esteves and Gijsbertus de With*[*]

Laboratory of Materials and Interface Chemistry,

Eindhoven University of Technology, Den Dolech 2, P.O. Box 513, 5600 MB

Eindhoven, The Netherlands.

* To whom correspondence should be addressed. E-mail: M.V.Villani@tue.nl;

G.deWith@tue.nl Phone: +31-40-2473132/+31-40-2474947.

Content:

S1. Thermal stability

The weight (%) versus temperature graphs obtained from TGA measurements are shown in Figure S1. From these graphs it was concluded that the coatings are thermally stable up to 200-250 °C. Therefore the DSC measurements were carried out up to 150 °C with no risk of degradation of the materials.

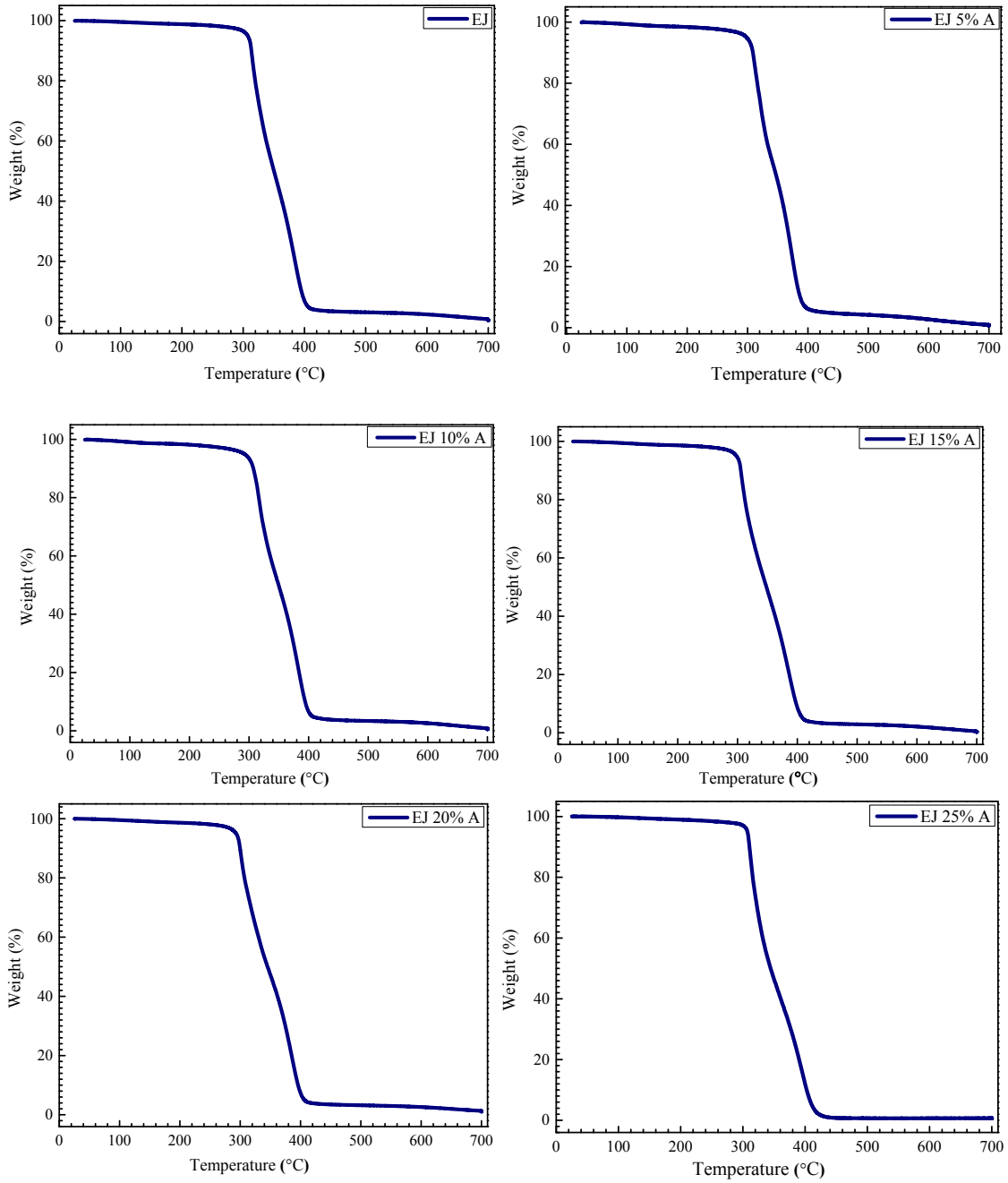

Figure S1. *TGA graphs showing the mass los (weight %) as a function of temperature.*

S2. The thermal treatment effect and its influence on stress/strain curves

In order to determine a possible thermal treatment effect on the mechanical properties of the materials, DMA measurements in 'multifrequency strain' mode were performed by subjecting the coatings to a thermal treatment at 100 °C for 1 hour before and after a stabilization period at 25 °C. The storage moduli of the samples were compared during these temperature cycles to understand the post-curing effect. Figure S2 depicts the effect of this thermal treatment.

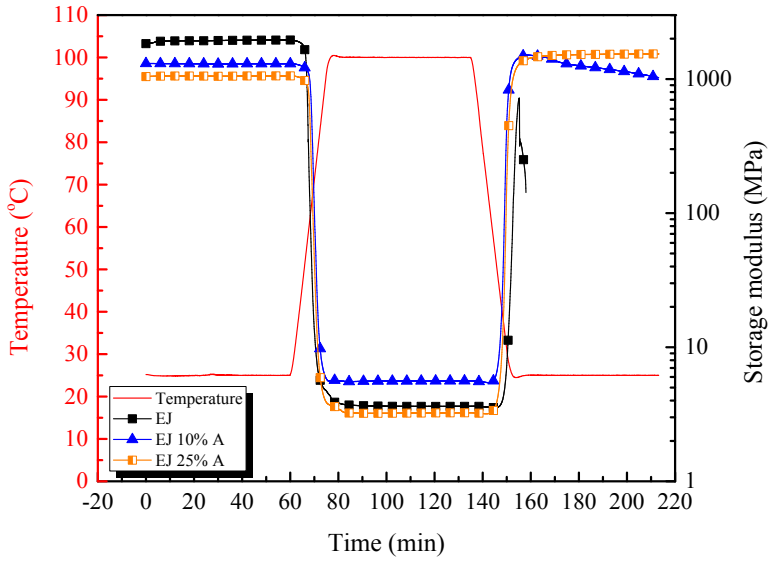

Figure S2. *The thermal treatment effect for EJ, EJ 10% A and EJ 25% A.*

For all samples, it was observed that the modulus values at room temperature before heating did not show any significant changes and are consistent with the values reported in Figure 4. This behavior is attributed to the similar stiffness of the samples due to being in glassy state. On the other hand, the modulus values changed after thermal treatment under the influence of post-curing. The modulus of the fully covalent network decreased from 1930 MPa to 720 MPa and the sample broke during the measurement because it became brittle due to internal stresses in the coating (possibly reinforced by stresses created by water desorption). The samples having 10% and 25% acetamide exhibited starting modulus values of 1304 and 1052 MPa, whereas there is a more pronounced difference after the thermal treatment at 100 °C, showing values of 1040 and 1540 MPa, respectively. The result belonging to EJ 25% A

seems to confirm the embrittlement of the material as a consequence of the thermal treatment effect.

To gain a better understanding of this embrittlement, controlled force measurements were carried out and the analysis was focused on the effect of thermal treatment time and temperature on E and ε_{yield} for different compositions. Figure S3 shows stress/strain curves of the samples kept at different time intervals.

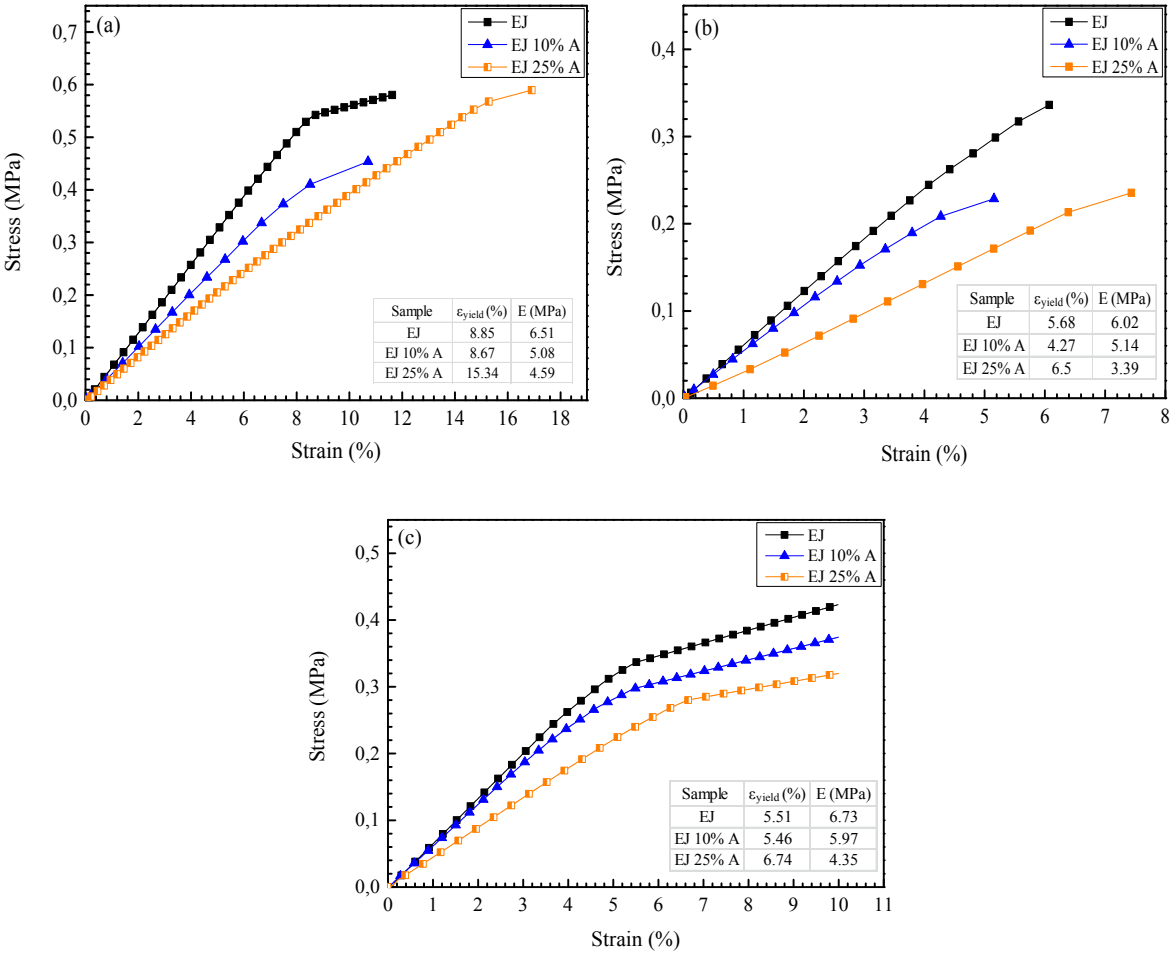

Figure S3. *Controlled force measurements to show how E and ε_{yield} change as a function of thermal treatment time. Samples were kept at 100 ℃ for (a) 5 min, (b) 30 min and (c) 2 hours.*

The thermal treatment temperature was chosen as 100 °C, which is the curing temperature used to prepare the samples. At 100 °C for 5 min, ≈ 9% of yield elongation was observed for the fully covalent material (EJ) with a modulus of 6.51 MPa, whereas for EJ 25% A 4.59 MPa and ≈ 15% of elongation was registered (Figure S3a).

At 100 °C for 30 min, the Young's moduli showed a similar trend where the fully covalent network has 6.0 MPa modulus and ~ 6% yield elongation. EJ 25% A exhibited a modulus of 3.4 MPa with an elongation of ≈ 6.5 % at yield point (Figure S3b).

Finally, at 100 °C for 2 hours, EJ has a Young's modulus of 6.7 MPa and an elongation of ≈ 5.5 % at yielding. On the other hand, EJ 25% A shows 4.4 MPa and elongates to ~ 7%. The values of EJ 10% A fall in between the values of the other two samples, with a modulus of 6.0 MPa (Figure S3c).

For all thermal treatment times, the fully covalent network shows lower ε_{yield} than EJ 25% A. Hence, this controlled force measurement confirms embrittlement, as also witnessed by previous DMA experiments. In addition to the illustration of stress/strain curves at elevated temperatures to show the thermal treatment effect, the measurements were also performed at room temperature (see Figure S4 and Table S1). The materials are in glassy state (see T_g's in Table 1) and the (low) upper force limit may have prevented following the continuation of the stress/strain curves after the elastic deformation. Therefore, the measurements at room temperature were shown to compare the Young's modulus of the samples. These values were determined again by controlled force mode and also were compared with the values obtained from multifrequency strain measurements, reported in Figure 4. Moreover, the linear viscoelastic region was determined for all samples.

A similar behavior in the mechanical properties of the materials was observed. This similarity is also in agreement with the results derived from the multifrequency strain mode of DMA carried out at room temperature. Secondly, the stress that would be applied for creep measurements was determined by checking Figure S3 and Figure 4S. According to the graphs, 0.1 MPa stress was convenient in order to be in the linear viscoelastic region.

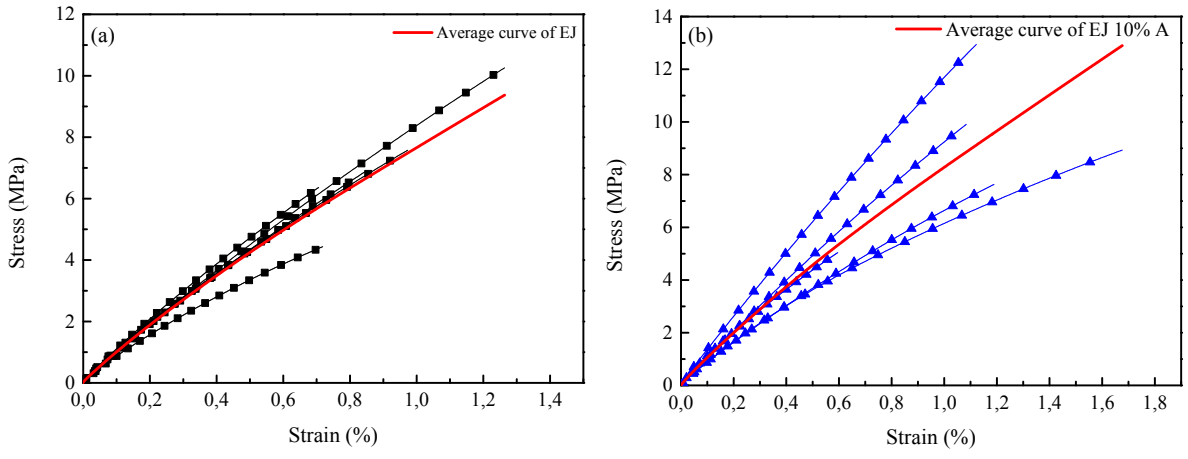

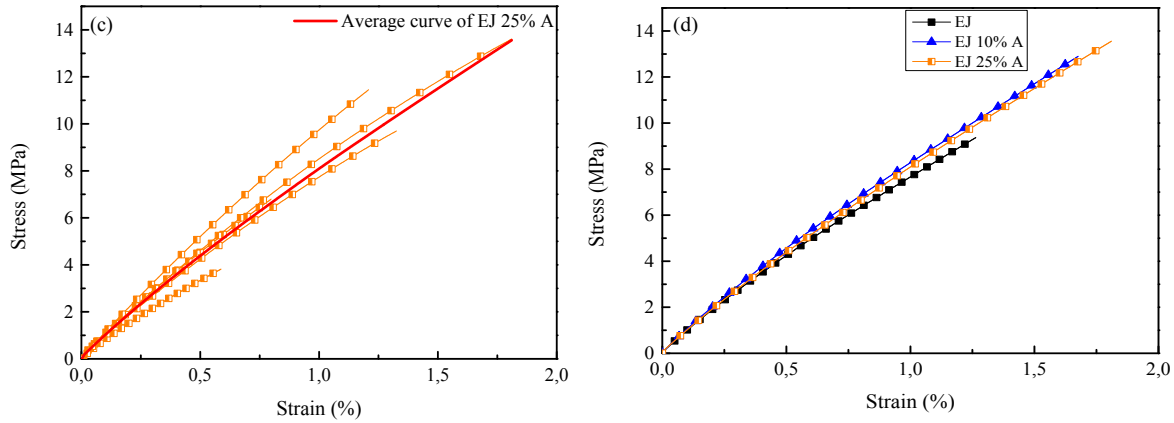

Figure S4. *Stress/strain curves at room temperature showing 5 measurements with their average curves for (a) EJ, (b) EJ 10% A, (c) EJ 25% A, and (d) Average values.*

Table S1. *Average Young's moduli obtained from Figure S4, where σ indicates the sample standard deviation.*

Sample	E_1 (MPa)	E_2 (MPa)	E_3 (MPa)	E_4 (MPa)	E_5 (MPa)	$E_{av.}$ (MPa)	σ (±)
EJ	809	800	890	609	765	774	103
EJ 10% A	916	1148	635	524	828	810	244
EJ 25% A	836	947	756	639	728	781	116

S3. Burgers Model fitting

The Burgers (or four parameters) model – a combination of Maxwell and Kelvin-Voigt elements – was employed to fit our experimental data. The Burgers model differential equation[1] reads $\dot{\varepsilon}_K + (k_K/\eta_K)\varepsilon_K = (1/\eta_K)\sigma$. Under a constant stress σ_0 we have:

$$\varepsilon(t) = \frac{\sigma_0}{k_M} + \frac{\sigma_0}{\eta_M}t + \frac{\sigma_0}{k_K}\left[1 - \exp\left(-\frac{k_K t}{\eta_K}\right)\right]$$

Here, t denotes time after loading, k_M and η_M are the modulus and viscosity of the Maxwell spring and dashpot, respectively, while k_K and η_K are the modulus and viscosity of the Kelvin spring and dashpot, respectively. The non-linear curve fit function of the OriginPro 7.5 software was used and the four parameters (k_M, k_K, η_M and η_K) were obtained (Figure S5), as summarized in Table S2.

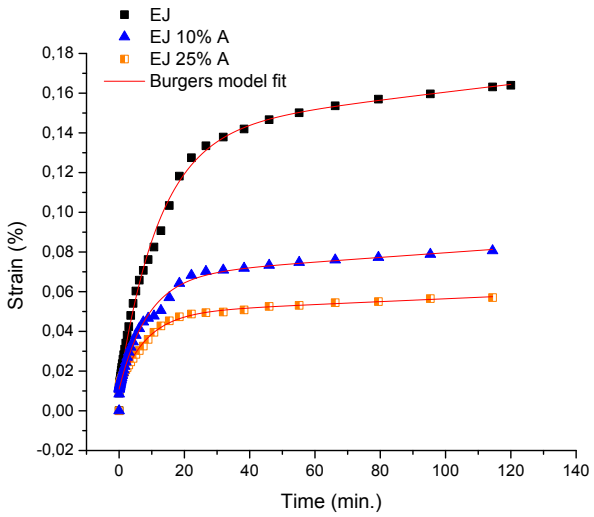

Figure S5. *Creep measurements at 0.1 MPa stress at 35 °C of films EJ, EJ 10% A, EJ 25 A%.*

Table S2. Parameters of the Burgers model for creep the measurements at 0.1 MPa stress at 35 °C of films EJ, EJ 10% A and EJ 25 A%.

Creep	k_M(MPa)	η_M(MPa·s)	k_K(MPa)	η_K(MPa·s)	τ(s)
EJ	8.25 ± 0.48	512 ± 105	0.77 ± 0.02	9.59 ± 0.30	12.5
EJ 10% A	9.25 ± 0.49	857 ± 222	1.75 ± 0.06	15.37 ± 0.83	8.8
EJ 25% A	8.47 ± 0.37	1380 ± 490	2.67 ± 0.12	22.4 ± 1.6	8.4

[1] G. de With, *Structure, deformation, and integrity of materials*, Wiley-VCH, Weinheim, 2006.

S4. Pull-off test

In Figure S9, a schematic of the pull-off set-up for the tests reported in the paper is given[2].

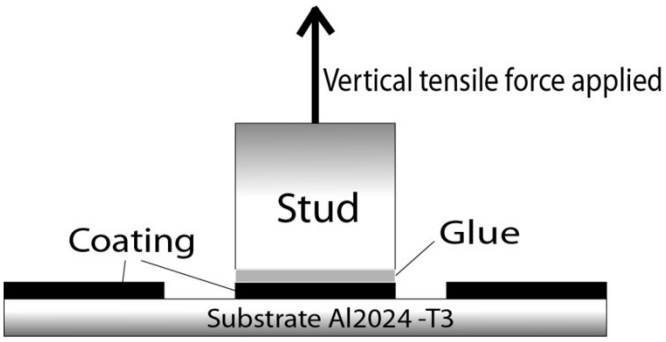

Figure S6. *Illustration of pull-off test.*

[2] Meis, N. N. A. H.; van der Ven, L. G. J.; van Benthem, R. A. T. M.; de With, G., Extreme wet adhesion of a novel epoxy-amine coating on aluminum alloy 2024-T3. *Prog Org Coat* **2014,** *77* (1), 176-183.

S5. Self-healing behavior

The degree of self-healing of the coatings was examined by under optical microscopy. An indentaion of width ≈ 200 μm and depth ≈ 60 μm was created with a well-defined cutter (see experimental) on bulk material of composition EJ 25% A. The progress of self-healing was monitored for 1 hour with 1 min intervals (Figure S6).

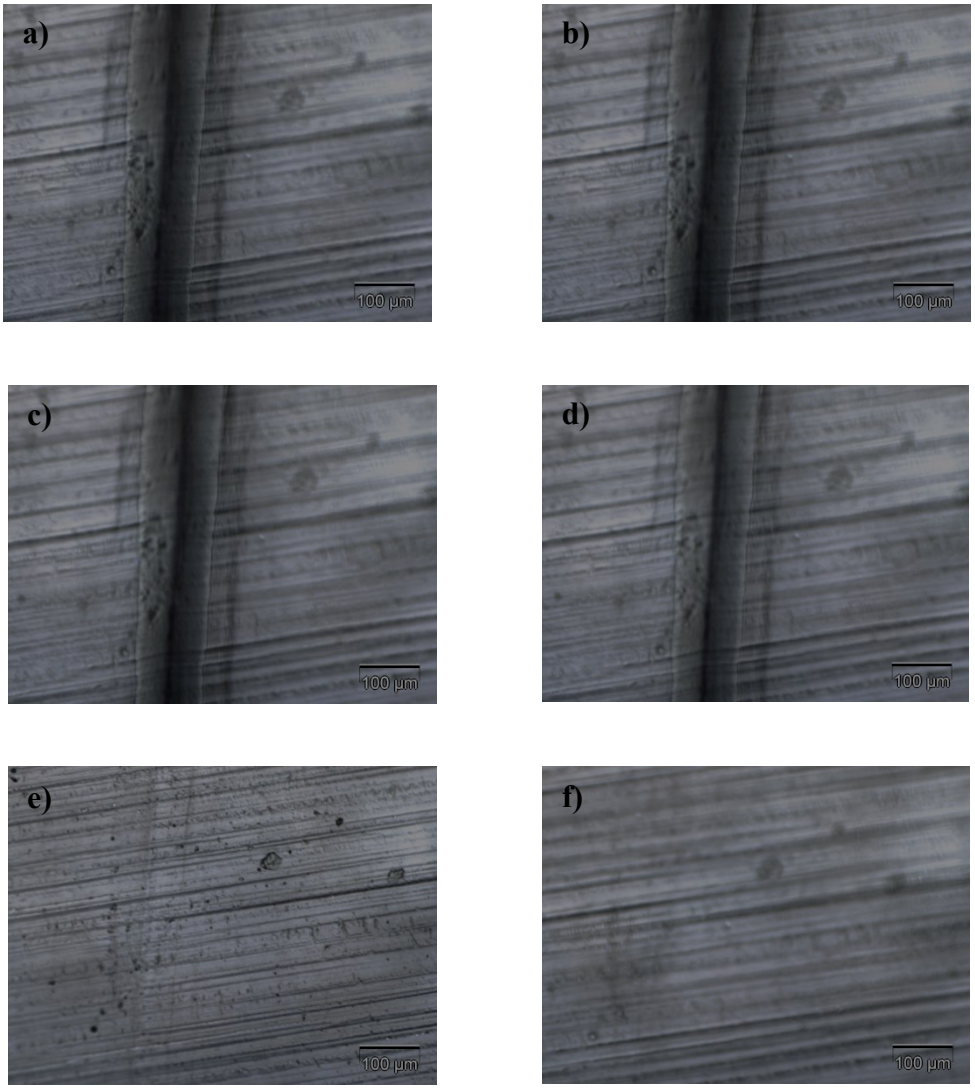

Figure S7. *Optical microscope images showing the healing process for EJ 25% A at T_g – 12 ℃ (45 °C) as a function of time after an indentation is formed. The images show the healing status at the centre of the indentation at a) 0 min, b) 2 min, c) 4 min, d) 6 min, e) 8 min, f) 10 min and g) 12 min.*

Material having only covalent cross-links was also tested applying the same procedure as mentioned for EJ 25% A. Figure S7 shows images taken at 10 min of intervals for 1 hour and, as expected, the indentation was not healed at all.

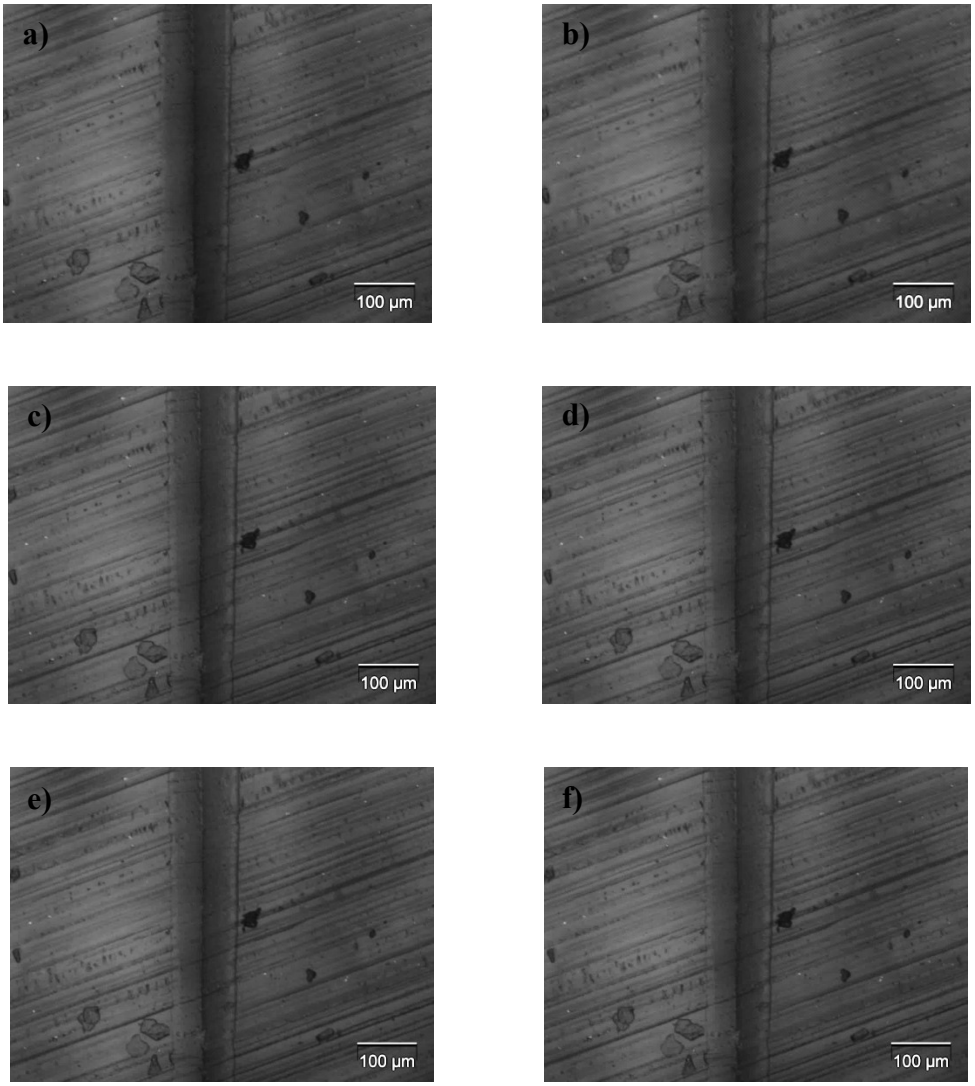

Figure S8. *Optical microscope images showing the healing process for the fully covalent material (EJ) at T_g – 12 ℃ (49 °C) as a function of time after an indentation is formed. The images show the healing status at the centre of the indentation at a) 0 min, b) 10 min, c) 20 min, d) 30 min, e) 40 min, f) 50 min and g) 60 min.*

To assess the progress of self-healing quantitatively, the depth and width of an indentation was also monitored using a cross-section of an indentation on material EJ 25% A for 1 hour with 1 min intervals at T_g – 12 °C (45 °C). Representative optical images are given in Figure

S8, while the relative depth and width as function of time are shown in Figure S9. As expected, a very similar behavior was observed, also showing complete healing in ≈ 10 min.

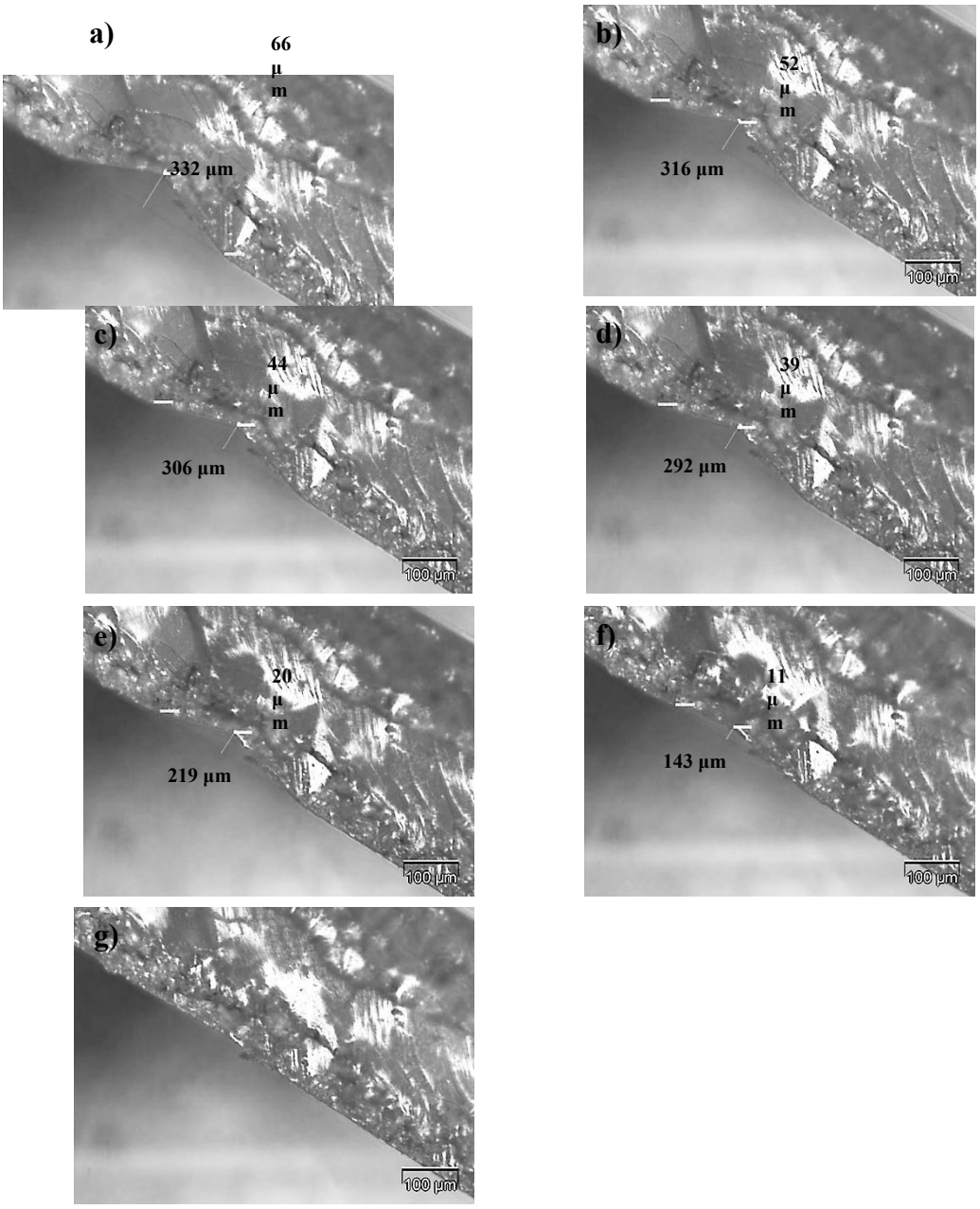

Figure S9. *Optical microscope images of an indentation showing the healing process for EJ 25% A at T_g – 12 ℃ (45 °C) at a) 0 min, b) 2 min, c)4 min, d) 6 min, e) 8 min, f) 10 min and g) 12 min.*

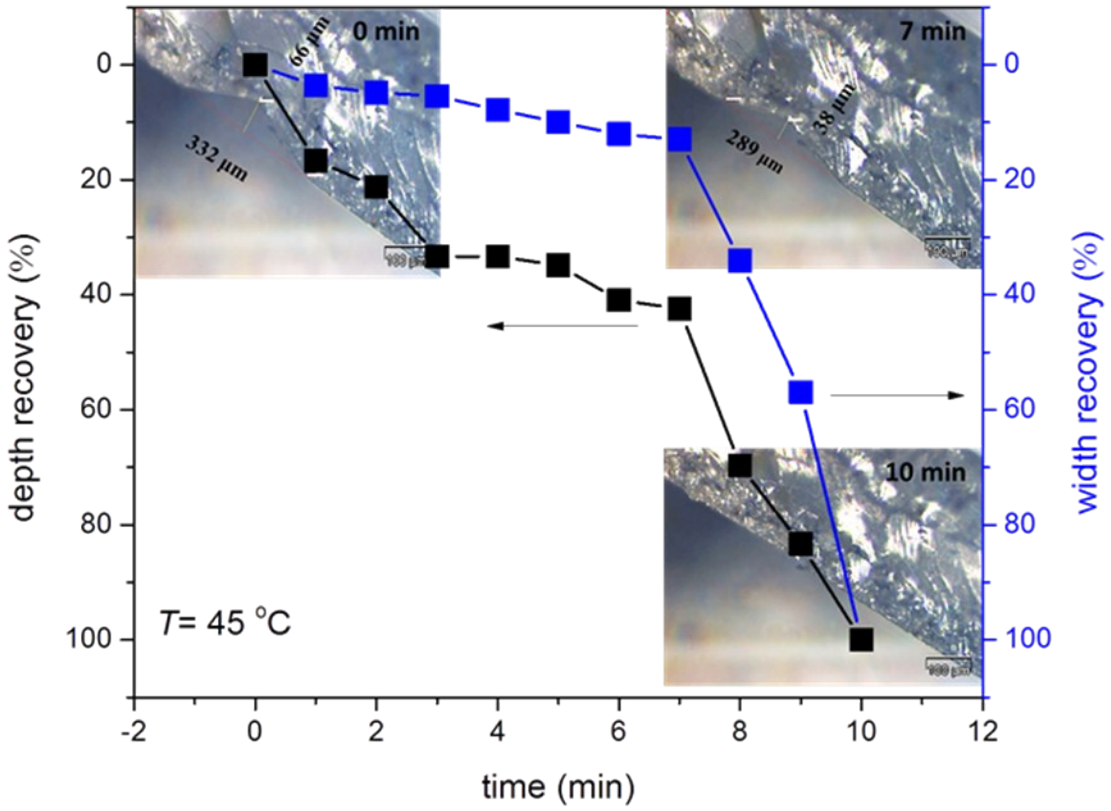

Figure S10. *A plot of the depth and width as function of time showing the healing process for EJ 25% A at* T_g *– 12 °C (45 °C), after an indentation is formed.*

S5. DMA RH experiments.

To investigate the cause of the increased T_g's values observed for both the EJ and the EJ 25% A materials after the indentation, some DMA RH experiments (dynamic mechanical analyzer under controlled humidity) were performed on EJ and the EJ 25% A cast films (15 × 5.1 × 1 mm^3). DMA temperature ramps were carried out in order to analyze further the effects observed previously. The ramps were conducted in linear tensile mode, after conditioning the samples for 300 mins at two different corresponding given relative humidity (Figures S11 a) and b)), from 5 °C to 105 °C. In particular a decrease of the T_g of 6 °C was observed for EJ by changing the RH from about 10% to 60%, and a decrease of the T_g of 9 °C for the EJ 25% A by a similar change of the RH (Figure S11). This suggested a significant influence of water on the properties and explained the different properties observed for these materials before and after healing. To confirm the water uptake effect on epoxy resins, the EJ 25% A was further analyzed by humidity (RH) controlled-DMA (dynamic mechanical analysis) under different controlled humidity levels, following the modulus of the material at a constant T of 60 °C (Figure S12). By changing the RH from about 10% to 60%, a decrease in modulus from about 1570 MPa to about 1053 MPa is observed in only 30 mins and a decrease from about 1570 MPa to about 729 MPa is observed in 60 mins (Table S3). A slower but not less significant variation is observed by changing the RH from about 60% to 10%. An increase of the modulus from about 127 MPa to about 165 MPa in 30 mins and from about 127 MPa to about 234 MPa is observed in 60 mins (Figure S13, Table S3). Although the water uptake effect on epoxy resins is well known, the change in modulus due to moisture is rather faster than previously observed in literature[3].

[3] See, e.g., N.J.W. Reuvers, H.P. Huinink, O.C.G. Adan, S.J. Garcia and J.M.C. Mol, Electrochimica Acta 94 (2013) 219– 228.

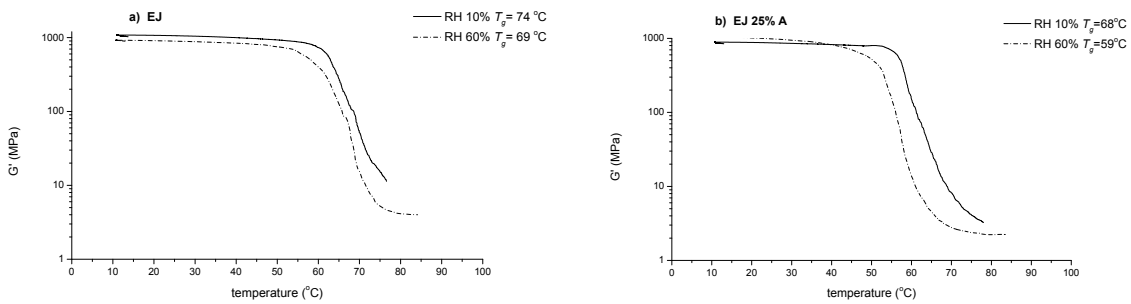

Figure S11. *Storage moduli as function of the temperature obtained via DMA temperature ramps conducted in linear tensile mode on EJ (a) and the EJ 25% A (b), after conditioning the samples for 300 mins at 10% and 60% Rh, respectively.*

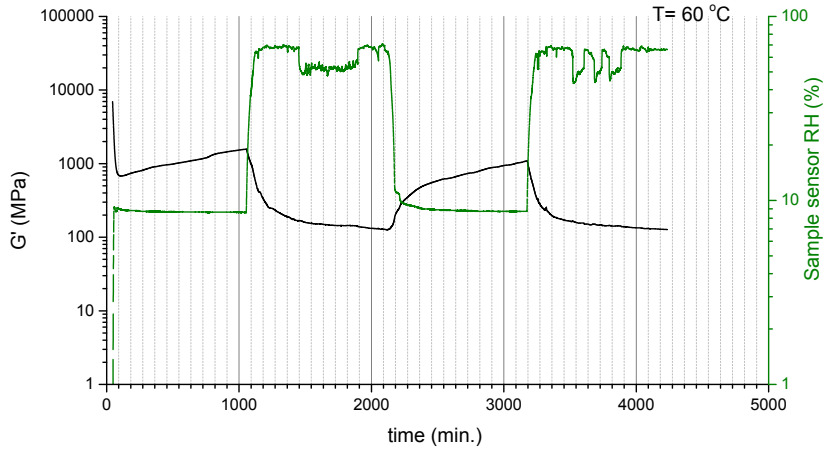

Figure S12. *Humidity (RH) controlled-DMA (dynamic mechanical analysis) on EJ 25% under different controlled humidity levels at a constant T of 60 ℃. The equilibration starts at t = 0 min, while the first humidity increase starts at 1055 min. The first humidity decrease starts at 2110 min.*

Table S3. Changes in modulus as a function of humidity for EJ 25% A.

Time	**Humidity 10% → 60%**	**Time**	**Humidity 60% → 10%**
	G′ (MPa)		*G′* (MPa)
0 min (1055 min)	1570	0 min (2110 min)	127
30 min (1085 min)	1053	30 min (2140 min)	165
60 min (1115 min)	729	60 min (2170 min)	234
2110 min	127	3165 min	1090